2020

Period-one Microwave Photonic Sensing by a Laser Diode with Optical Feedback

Bairun Nie
University of Wollongong, bn807@uowmail.edu.au

Yuxi Ruan
University of Wollongong, yr776@uowmail.edu.au

Yanguang Yu
University of Wollongong, yanguang@uow.edu.au

Qinghua Guo
University of Wollongong, qguo@uow.edu.au

Jiangtao Xi
University of Wollongong, jiangtao@uow.edu.au

See next page for additional authors

Period-one Microwave Photonic Sensing by a Laser Diode with Optical Feedback

Abstract

With external optical feedback (EOF), a laser diode (LD) can operate at different dynamic states. In this work, an LD with EOF is set at period-one (P1) oscillation state to generate microwave photonic (MWP) signal for sensing. Firstly, the P1 state boundary of the LD is determined and then the influence of the LD controllable parameters on the boundary is studied by solving the well-known Lang-Kobayashi equations. A set of parameters selection rule for designing an LD based MWP sensing system is obtained. In addition, a measurement algorithm for recovering the displacement from an MWP sensing signal is developed. By making full use of the sensing information carried in both amplitude and frequency of the MWP signal, displacement sensing with high resolution and large range can be achieved. Both simulations and experiments are conducted to verify the proposed method and show it is capable of realizing wide measurable range, high measurement sensitivity, and high resolution sensing.

Keywords

microwave, photonic, sensing, period-one, laser, feedback, diode, optical

Disciplines

Engineering | Science and Technology Studies

Publication Details

B. Nie, Y. Ruan, Y. Yu, Q. Guo, J. Xi & J. Tong, "Period-one Microwave Photonic Sensing by a Laser Diode with Optical Feedback," Journal of Lightwave Technology, 2020.

Authors

Bairun Nie, Yuxi Ruan, Yanguang Yu, Qinghua Guo, Jiangtao Xi, and Jun Tong

Period-one Microwave Photonic Sensing by a Laser Diode with Optical Feedback

Bairun Nie, Yuxi Ruan, Yanguang Yu, *Senior Member, IEEE*, Qinghua Guo, *Senior Member, IEEE*, Jiangtao Xi, *Senior Member, IEEE*, and Jun Tong, *Member, IEEE*

***Abstract*—With external optical feedback (EOF), a laser diode (LD) can operate at different dynamic states. In this work, an LD with EOF is set at period-one (P1) oscillation state to generate microwave photonic (MWP) signal for sensing. Firstly, the P1 state boundary of the LD is determined and then the influence of the LD controllable parameters on the boundary is studied by solving the well-known Lang-Kobayashi equations. A set of parameters selection rule for designing an LD based MWP sensing system is obtained. In addition, a measurement algorithm for recovering the displacement from an MWP sensing signal is developed. By making full use of the sensing information carried in both amplitude and frequency of the MWP signal, displacement sensing with high resolution and large range can be achieved. Both simulations and experiments are conducted to verify the proposed method and show it is capable of realizing wide measurable range, high measurement sensitivity, and high resolution sensing.**

***Index Terms*—Displacement measurement, microwave photonics, laser dynamics, laser sensing, optical feedback.**

I. Introduction

LASER diode (LD) attracts much attention from researchers due to its small size, low cost in manufacturing, and operate at low power consumption. It has been found that external optical feedback (EOF) can significantly affect the properties and behaviors of an LD [1, 2]. Regarding the EOF effect in an LD, on one hand, researchers try to avoid or eliminate the influence of EOF on an LD. On the other hand, researchers actively make full use of EOF for sensing and instrumentation. For example, utilizing LD with EOF contributes to the discovery of a new class of laser interferometry which is named as optical feedback interferometry (OFI) or self-mixing interferometry (SMI) [3]. The principle of such interferometer and the physical process is that, when a portion of the light is back-scattered or back-reflected by an external target and re-enter the LD internal cavity, both laser intensity and its frequency can be altered by the movement information associated with the target. The schematic structure of a typical LD with EOF sensing system is depicted in Fig. 1, it consists an LD, a photodiode (PD), a focusing lens and an external target. Under the different operational conditions, the LD undergoes from steady (S) state, period-one (P1) oscillation, quasi-period (QP) oscillation to chaos (C) [4]. Various potential applications have been investigated and reported in different dynamic states. In steady state, an LD with EOF can be utilized to detect the Doppler shift, vibration, velocity measurement, and displacement [5-8]. In P1 state, the optical injection and optical feedback schemes were used to generate microwave [9-11]. In work [9], a periodic switching between two nonlinear dynamic states caused by optical feedback is demonstrated. By adjusting the feedback strength, the duty cycle of the periodic state can be adjusted, thereby a tunable method for generating microwave photonic (MWP) signal is proposed. In work [10], a method of generating reconfigurable radar waveform based on optical injection is presented. In this method, a low-speed control signal is used to adjust the injection strength so that to control the output microwave frequency. The work [10] experimentally proved that the proposed microwave generator can be used for radar applications. Other applications for MWP include MWP processing, sensing, and fiber-optic radio communication [12-17]. In quasi-period state, LD with the influence from EOF will generate subwavelength, by monitoring frequency shift can achieve multi-dimensional 2D measurement [18]. In chaos, due to the broad bandwidth and pseudo-randomness of chaotic oscillation, it can be implemented in chaotic radar and chaotic secure communication [19, 20], et al.

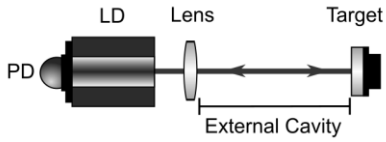

Fig. 1.Schematic structure of an LD with EOF system for sensing.

An LD with EOF sensing system operates at steady state (that is OFI/SMI) can provide a displacement measurement resolution with half laser wavelength ($\lambda_0/2$). For further improving the sensing resolution, one group of researchers make use of OFI sensing model to retrieve displacement from an OFI waveform [21, 22]. Theoretically, this method can achieve super high resolution. However, due to inevitable intensity noise and inaccurate model parameters, the resolution is still very limited, e.g., the work in [21] declared that $40nm$

Manuscript received January 27, 2020; revised April 14, 2020; accepted May 5, 2020. (*Corresponding author: Yanguang Yu.*)

The authors are with the School of Electrical, Computer and Telecommunications Engineering, University of Wollongong, NSW 2522, Australia. (e-mail: bn807@uowmail.edu.au; yr776@uowmail.edu.au; yanguang@uow.edu.au; qguo@uow.edu.au; jiangtao@uow.edu.au; jtong@uow.edu.au).

resolution can be achieved experimentally. Another group of researchers modulate the LD injection current or external cavity to have the displacement to be carried in the phase of an OFI signal, e.g., the work in [23] achieves a resolution of $15nm$ in experiment by retrieving the initial phase using fast Fourier transform (FFT). It requires a target to be measured must be in a low speed relative to the modulation period and the measurement range is about $1\mu m$. The work in [24] added extra physical components and combined the high sensitivity of a frequency-shifted feedback laser with the axial positioning capability of a confocal microscope, it reached $2nm$ resolution with about $10\mu m$ measurement range. Our work in [25] proposes to set the LD in an OFI sensing system operating at P1 state to generate MWP signal for sensing. This can provide a resolution of $\lambda_0/1280$ theoretically. And our recent work in [26], an LD with dual-cavity EOF operating at P1 state was proposed to deal with the target has a low reflectivity by utilizing MWP signal. It demonstrated the measurement sensitivity can be boosted up to 268 times compared to a general OFI/SMI sensing. However, how to design an LD with EOF system that can robustly working at P1 state to generate MWP signal and what is the applicable measurable range are not discussed in previous studies.

In this paper, we propose to improve the sensing performance for an LD based MWP sensing system in terms of measurement resolution, sensitivity, and measurable range. We first determine the P1 region boundaries for an LD with EOF system and study the P1 boundaries characteristics. Then, we investigate how the system controllable parameters influence the P1 boundaries, from which a set of parameters selection rules are presented. As an application example, an experimental displacement sensing system is investigated.

II. Determine P1 Region and Its Influence Parameters

The dynamic behaviors of an LD with EOF can be described by the well-known Lang-Kobayashi (L-K) equations [1].

$$\frac{dE(t)}{dt}=\frac{1}{2}\left\{G\left[N(t),E(t)\right]-\frac{1}{\tau_p}\right\}E(t)+\frac{\kappa}{\tau_{in}}\cdot E(t-\tau)\cdot\cos\left[\omega_0\tau+\phi(t)-\phi(t-\tau)\right] \tag{1}$$

$$\frac{d\phi(t)}{dt}=\frac{1}{2}\alpha\left\{G\left[N(t),E(t)\right]-\frac{1}{\tau_p}\right\}-\frac{\kappa}{\tau_{in}}\cdot\frac{E(t-\tau)}{E(t)}\cdot\sin\left[\omega_0\tau+\phi(t)-\phi(t-\tau)\right] \tag{2}$$

$$\frac{dN(t)}{dt}=\frac{J}{eV}-\frac{N(t)}{\tau_s}-G\left[N(t),E(t)\right]E^2(t) \tag{3}$$

In above equations, there are three variables named as electric field amplitude $E(t)$, electric field phase $\phi(t)$ and carrier density $N(t)$. $\phi(t)$ is given by $\phi(t)=[\omega(t)-\omega_0]t$, where $\omega(t)$ is the instantaneous optical angular frequency for an LD with optical feedback, ω_0 is the unperturbed optical angular frequency for a solitary LD. $G[N(t),E(t)]=G_N[N(t)-N_0][1-\varepsilon\Gamma E^2(t)]$ is the modal gain per unit time. The physical meanings of the symbols appearing in (1)-(3) and the values of the parameters used in this paper can be found in Table I [25]. Through numerically solving above L-K equations, the laser intensity $E^2(t)$ can be obtained, $E^2(t)$ is also called sensing signal. The LD dynamic states can be identified by observing the waveform of $E^2(t)$. Under the proper external perturbations, the system can enter P1 dynamics through Hopf bifurcation with undamped relaxation resonance of the LD [4]. To determine the P1 region and study its features, we present all the dynamic states of an LD in the coordinate plane of (L, κ), each state on the (L, κ) plane is determined by both internal and external parameters of the LD. The internal parameters are fixed for a certain LD but the injection current (J) and line-width enhancement factor (α) may varies when designing a system. Thus, there is a need to study how these two parameters influence the P1 region, from which we can determine an optimal P1 region for sensing.

TABLE I
PHYSICAL MEANING OF ALL SYMBOLS IN (1)-(3)

	Symbol	Physical Meaning	Value
LD Internal Parameters	G_N	Model gain coefficient	$8.1\times10^{-13}\text{m}^3\text{s}^{-1}$
	N_0	Carrier density at transparency	$1.1\times10^{24}\text{m}^{-3}$
	ε	Nonlinear gain compression coefficient	$2.5\times10^{-23}\text{m}^3$
	Γ	Confinement factor	0.3
	τ_p	Photon lifetime	$2.0\times10^{-12}\text{s}$
	τ_s	Carrier lifetime	$2.0\times10^{-9}\text{s}$
	τ_{in}	Internal cavity round-trip time	$8.0\times10^{-12}\text{s}$
	e	Elementary charge	$1.6\times10^{-19}\text{C}$
	V	Volume of the active region	$1\times10^{-16}\text{m}^3$
	ω_0	Angular frequency of solitary laser, $\omega_0=2\pi c/\lambda_0$, where c is the speed of light, λ_0 is the wavelength of the LD	
	α	Line-width enhancement factor	
LD Extemal Parameters	J	Injection current	
	κ	Feedback strength	
	L	External cavity length	
	τ	Light round-trip time in the external cavity, $\tau=2L/c$	

m = meter, s = second, C = coulomb

Firstly, we study the influence of injection current J on the P1 region. Fixing line-width enhancement factor with $\alpha=3$, we set injection current with $J=1.1J_{th}$, $J=1.3J_{th}$, and $J=1.5J_{th}$ respectively, where J_{th} is the threshold of the injection current. For each case, we vary the external cavity length L which travels from $0mm$ to $500mm$ with a step of $\Delta L=5mm$. At each L, we increase feedback strength κ from 0 to 0.04 with step of $\Delta\kappa$=0.0001 and finer when close to the state boundaries, then using L-K equations to generate

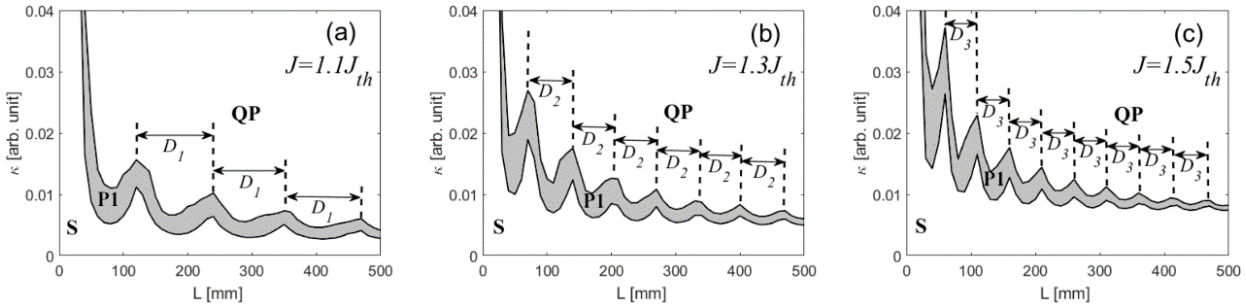

Fig. 2. Influence of J on the P1 region with $\alpha = 3$. (a) $J = 1.1J_{th}$ and $D_1 = 120mm$. (b) $J = 1.3J_{th}$ and $D_2 = 70mm$. (c) $J = 1.5J_{th}$ and $D_3 = 50mm$.

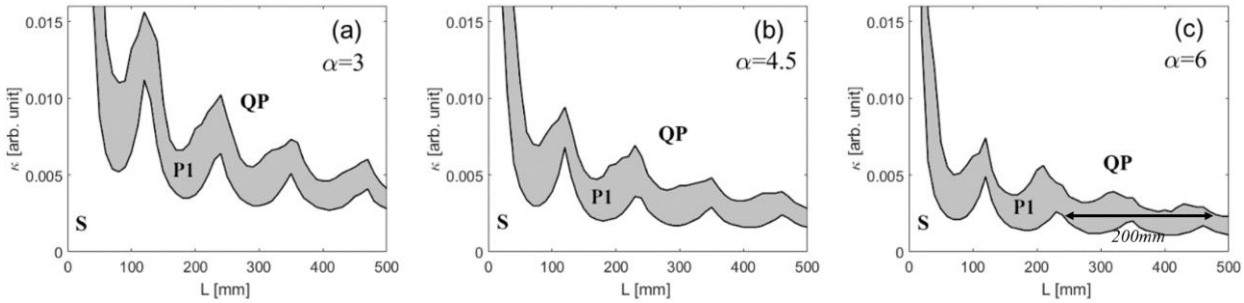

Fig. 3. Influence of α on the P1 region with $J = 1.1J_{th}$. (a) $\alpha = 3$. (b) $\alpha = 4.5$. (c) $\alpha = 6$.

$E^2(t)$ for every κ value. For each given set of parameters, we record the corresponding LD state on the (L, κ) plane. The LD states diagrams are obtained and shown in Fig. 2, where the P1 region is the shaded area. It can be seen, the P1 region is a fluctuated band with an approximately modulation period denoted by D along L direction. At a suitable κ value, with the changes of L, the system switches between steady state and P1 state. This provides the possibility to implement a tunable optical microwave generator.

The approximate modulation periods D are shown on Fig. 2, with $D_1 = 120mm$, $D_2 = 70mm$, and $D_3 = 50mm$, it indicates the modulation periods are decreasing with increasing of J. Each case also shows that the P1 region with a slight downward trend, which indicates the shorter the external cavity is, the higher κ is required to maintain the LD in P1 state. With the length of the external cavity increases, a lower feedback strength will cause the system switching between S and P1 state periodically. Furthermore, an increasing J causes narrower band of P1 region and move the band location to the high κ level. This will make the LD more difficult to be kept within P1 region.

Then, we investigate the influence of line-width enhancement factor α on the P1 region. We set three different line-width enhancement factors as $\alpha = 3$, $\alpha = 4.5$, and $\alpha = 6$, with a fixed injection current at $J = 1.1J_{th}$. The results are shown in Fig. 3. It can be seen that α has a strong influence on the P1 region for $L < 300mm$. A large α leads to a low κ level is required to be maintained in P1 state, the overall P1 region tends flatter with increasing α. Therefore, an LD with a large line-width enhancement factors α is more likely to operate at P1 region.

III. Utilizing P1 Region for Sensing

Based on the study of the P1 region in above, a low J and a relative large α are adopted to obtain a wide P1 region as show in Fig. 3(c), an operating range is indicated up to about $200mm$. With this knowledge, we can operate an LD at a stable P1 state. Therefore, for the following simulations, we set $J = 1.1J_{th}$, $\alpha = 6$, $L = 300mm$. Through solving L-K equations, a bifurcation diagram for the LD can be obtained and shown in Fig. 4. A relative laser intensity $I(t)$ is used to represent the MWP sensing signal, we define $I(t) = E^2(t) / E_0^2$, where E_0^2 is the laser intensity without optical feedback. It can be seen in the range from κ=0.00125 to κ=0.00357, we can guarantee the LD with EOF operating at P1 state. To test the sensing performance for this system, we set $J = 1.1J_{th}$, $\alpha = 6$, $L = 300mm$, κ=0.0025, and assume the external target has a linear displacement $\Delta L = 0.8\lambda_0 t$, through numerically solving the L-K equations, the MWP sensing signal in P1 state and external target movement ΔL are shown in Fig. 5. From Fig. 5, we found the $I(t)$ contains rich information related to the target displacement. The MWP sensing signal operating in the P1 region has a high frequency oscillation locating at $1.3GHz$ with its amplitude modulated by a slow varying signal. This oscillate frequency is called as relaxation oscillation frequency (denoted by f_R). The envelop of $I(t)$ is periodically repeated with a period corresponding to $\lambda_0 / 2$, we call each period as an integer fringe. By counting the integer number of fringes (denoted by M), we can achieve a coarse measurement (denoted by ΔL_i) by (4).

$$\Delta L_i = \frac{\lambda_0}{2} \cdot M \tag{4}$$

We further study the characteristics for the high frequency oscillation component of $I(t)$. Given ΔL changes from 0 to $1.5\lambda_0$ with a step of $0.01\lambda_0$. For each given ΔL, $E^2(t)$ is generated through solving L-K equations and then perform FFT on the $E^2(t)$ to determine its f_R, the relationship between f_R and ΔL shown in Fig. 6.

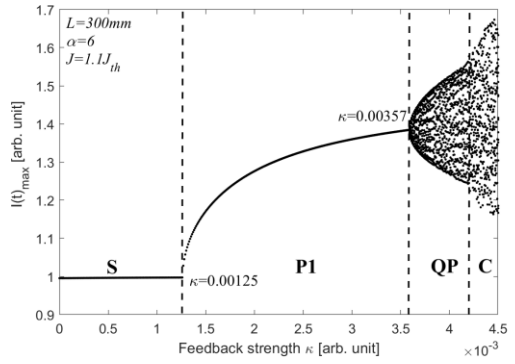

Fig. 4. Bifurcation diagram for an LD with EOF system, $J = 1.1J_{th}$, $\alpha = 6$, and $L = 300mm$.

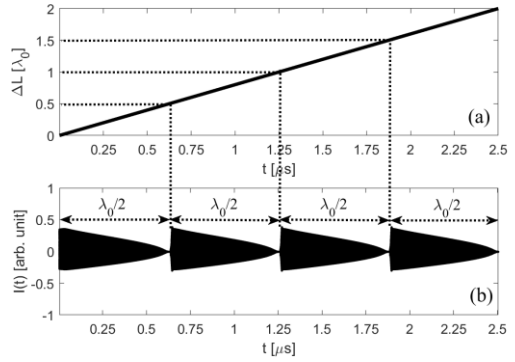

Fig. 5. Utilizing P1 region for sensing. (a) Displacement of external target. (b) Corresponding MWP sensing signal in P1 region.

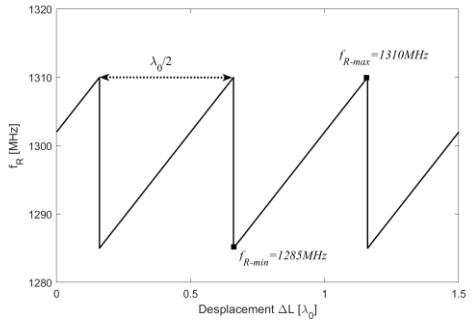

Fig. 6. Relationship between f_R and ΔL.

From Fig. 6, we found that the oscillation frequency is also time varying with a periodically change period of $\lambda_0/2$, within each period ($0 < \Delta L < \lambda_0/2$), there is a linear relationship between f_R and ΔL with a conversion slope $k_s = (f_{R-\max} - f_{R-\min})/(\lambda_0/2)$. This linear relationship enables us to develop a sensing method to measure the fractional fringe (denoted by ΔL_f) by using f_R. Therefore, a fine measurement for target displacement less the $\lambda_0/2$ can be made by (5), where, $f_{R-start}$ is the f_R corresponding to the $E^2_{start}(t)$ recorded at the initial position of the target, and f_{R-end} is the f_R corresponding to the $E^2_{end}(t)$ recorded at the end position of the target. The displacement resolution for the fractional fringe measurement depends on frequency analysis device. For example, the Tektronix RSA5000 series spectrum analyzer can set resolution bandwidth (RBW) from $100Hz$ to $5MHz$, if we adopt an spectrum analyzer with spectrum resolution of $1MHz$ to record f_R, in the case of Fig. 6, conversion slope $k_s = 0.064MHz/nm$, therefore, we can get a sensing resolution of $15.6nm$ ($\lambda_0/50$, where $\lambda_0 = 780nm$). For further improving the sensing resolution, if a spectrum analyzer with spectrum resolution of $62.5KHz$ is employed. With the same conversion slope $k_s = 0.064MHz/nm$, the resolution can reach up to $0.98nm$ ($\lambda_0/799$, where $\lambda_0 = 780nm$).

$$\Delta L_f = \frac{f_{R-end} - f_{R-start}}{k_s} \tag{5}$$

As indicated in Fig. 4, the feedback strength κ can be adjusted to different values within P1 region. Fig. 7 shows the extracted envelopes of MWP sensing signals $I(t)$ (denoted by $I(t)_{Envelope}$) corresponding to different feedback strength with $\kappa = 0.0020$, $\kappa = 0.0025$, and $\kappa = 0.0030$, respectively. It can be seen that a high feedback strength is recommended since its corresponding MWP sensing signal $I(t)$ can achieve a larger magnitude. This means a higher sensitive sensing can be achieved.

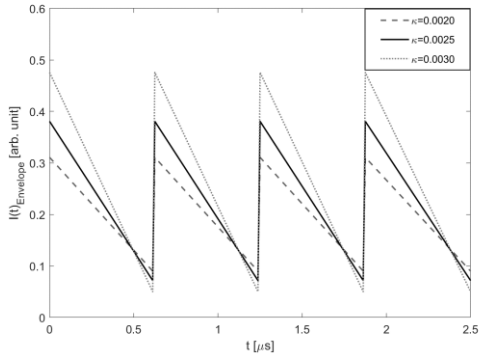

Fig. 7. Waveform of $I(t)_{Envelope}$ under different feedback strength.

IV. EXPERIMENT

The above analysis shows the LD with EOF operate in P1 state can be used in displacement sensing, we are able to achieve both integer and factional fringe measurements. To verify the proposed approach, an experiment is set up and depicted in Fig. 8. The LD is a single mode (Hitachi, HL8325G, $\lambda_0 = 830mm$, maximum output power $P_0 = 40mW$) and is driven by an LD controller (Thorlabs, ITC4001) with an injection threshold current of $J = 42mA$ and operating

temperature at $T = 24 \pm 0.01^{\circ}C$. An external target (mirror) is attached to a piezoelectric (PZT) actuator (PI, P-841.2) and then installed on a linear stage (Thorlabs, NRT100/M) to move the target at different position with a range up to $100mm$. The target is driven by a PZT actuator to have a small displacement range up to $30\mu m$. A variable attenuator (VA) is used to adjust optical feedback amount to enter the LD. A beam splitter (BS) with a splitting ratio of $50:50$ is employed to direct a part of light into an external PD (Thorlabs, PDA8GS) with a bandwidth of $9.5GHz$. A high speed digital oscilloscope (Tektronix, DSA70840) with a maximum sampling rate of $25GHz$ and analog bandwidth of $8GHz$ is used. The oscilloscope can be utilized to observe output waveform of the MWP sensing signal $E^2(t)$ and perform FFT on the sensing signal.

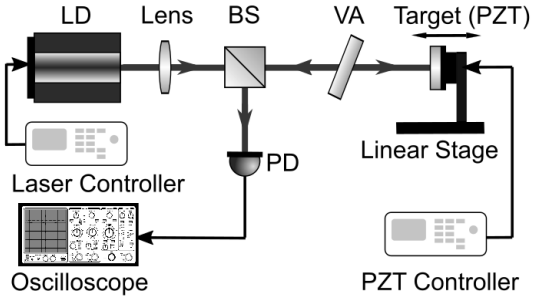

Fig. 8. Experiment set-up.

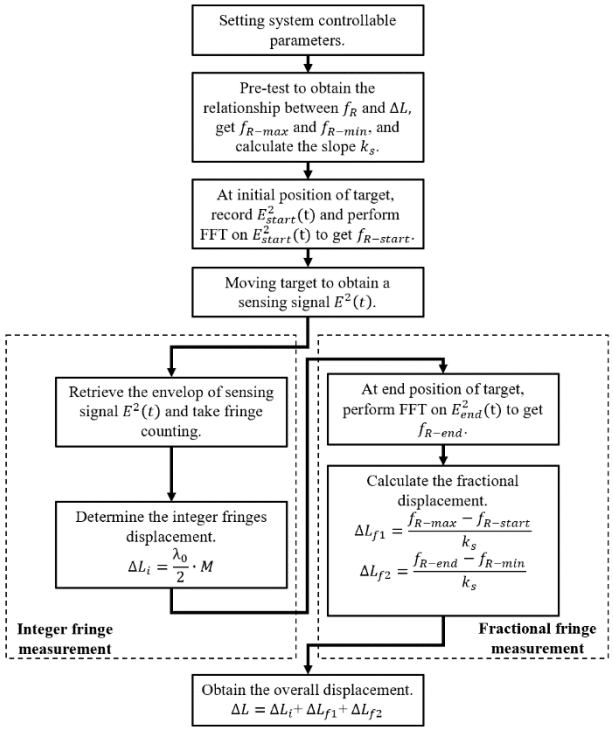

Fig. 9. Measurement procedure of the proposed approach.

The measurement procedure is presented by the flowchart shown in Fig. 9. The details of the main steps in measurement procedure are described as following:

First, we need experimentally determine the P1 region for our physical system. Based on the theoretical study in Section II, we give a low injection current $J = 1.1J_{th}$ (46.2mA), and tested a few LDs, the α factor in the LDs can be calculated by utilizing the methods that we proposed in [27], and choose the LD with $\alpha = 4$, the external cavity length $L = 300mm$. We adjust the VA to obtain a suitable feedback strength to ensure sensing system can maintain at P1 state over the whole measurement range.

Second, apply $20nm$ displacement as step size on the PZT each time. For each step, observe the MWP sensing signal $E^2(t)$ from oscilloscope and ensure system operates in the P1 oscillation, then record its displacement ΔL and the corresponding relaxation oscillation frequency f_R through FFT function provided by the oscilloscope, we establish the relationship between f_R and ΔL as the pre-test. The pre-test experimental results are shown in Fig. 10, it elucidates a linear relationship between f_R and ΔL with a conversion slope of $0.174MHz/nm$, and we also record the value of $f_{R-\max}$ and $f_{R-\min}$ in Fig. 10.

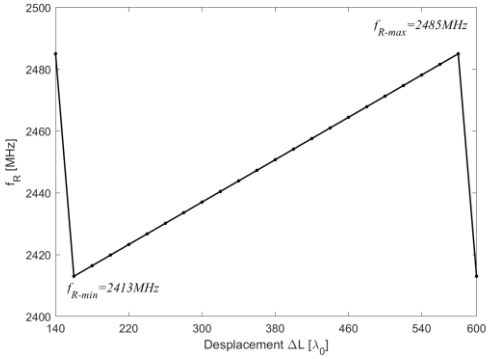

Fig. 10. Pre-test results for the relationship between f_R and ΔL with $J = 1.1J_{th}$ (46.2mA), $L = 300mm$, and $\alpha = 4$.

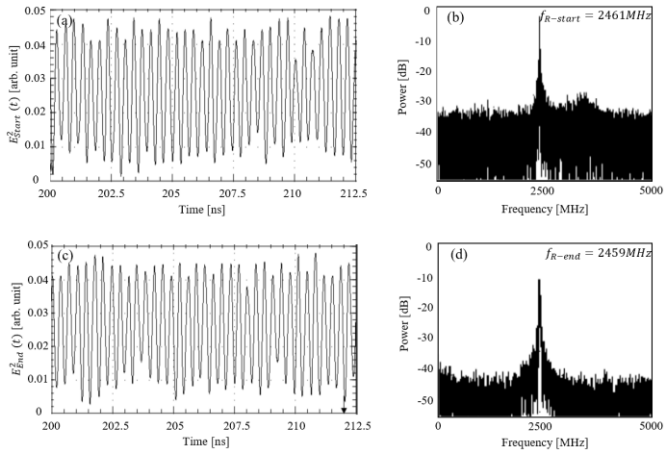

Fig. 11. Experiment results. (a) MWP sensing signal $E^2_{start}(t)$ at initial position of target. (b) Spectrum corresponding to the $E^2_{start}(t)$. (c) MWP sensing signal $E^2_{end}(t)$ at end position of target. (d) Spectrum corresponding to the $E^2_{end}(t)$.

Third, at the target initial position, we record the MWP sensing signal $E^2_{start}(t)$, then perform FFT on $E^2_{start}(t)$ to get $f_{R-start} = 2461MHz$, the MWP sensing signal $E^2_{start}(t)$ in P1

oscillation and its corresponding spectrum are given in Fig. 11(a)-(b). A PZT controller is used to drive the target in a linear movement with $2072nm$ displacement and the linearity of the signal up to 0.15% , by generating a ramp driving voltage signal of $7V$ and apply it on PZT, shown in Fig. 12(a). Fig. 12(b) gives the corresponding MWP sensing signal $E^2(t)$ in P1 region, which experimentally recorded by the oscilloscope. It can be seen that there are four integer fringes in total, which corresponding to $\Delta L_i = \frac{\lambda_0}{2} \cdot 4 = 1660nm$, where $\lambda_0 = 830nm$.

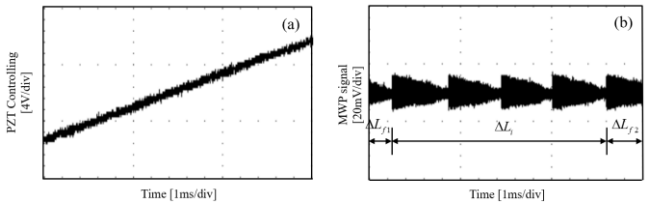

Fig. 12.(a) A linear displacement applied on target by PZT. (b) The corresponding MWP sensing signal.

When the target stop displacement at the end position, record the MWP sensing signal $E_{end}^2(t)$ shown in Fig. 11(c), by performing FFT on the $E_{end}^2(t)$ to determine $f_{R-end} = 2459MHz$, the MWP sensing signal $E_{end}^2(t)$ in P1 oscillation and its corresponding spectrum are given in Fig. 11(c)-(d). Then we start fractional measurement. For example, in order to determine the displacement of ΔL_{f1} , the starting frequency $f_{R-start} = 2461\text{M}Hz$ can be get from Fig. 11(b), and $f_{R-end} = f_{R-\max} = 2485MHz$, according (5), we can easily get $\Delta L_{f1} = 137.93nm$. Similarly, for ΔL_{f2} , $f_{R-end} = 2459MHz$ can be seen from Fig. 11(d), and $f_{R-start} = f_{R-\min} = 2413MHz$, we can calculate $\Delta L_{f2} = 264.37nm$. Therefore, the overall displacement is $\Delta L = \Delta L_i + \Delta L_{f1} + \Delta L_{f2} = 2062.30nm$, which is closed to the pre-set displacement value of PZT. The RBW of the high speed digital oscilloscope in this experiment is $62.5KHz$, which is adopted to record relaxation oscillation frequency f_R . The variation of f_R within a fringe is $72MHz$. If we can guarantee a perfect linear slope shown in Fig 10, a resolution of $0.36nm$ ($\lambda_0 / 2304$, where $\lambda_0 = 830nm$) for position sensing can be achieved. It can be seen that the obtained resolution by employing the LD with EOF system operates at P1 state, which provides much higher resolution compare to the traditional OFI/SMI.

V. Conclusion

In this paper, we studied the dynamic state boundaries of the P1 state in an LD with EOF system. The effect of external cavity length L , feedback strength κ , injection current J , and line-width enhancement factor α on the boundary of the P1 state are investigated. Our study found that a low J , a relative large α , and a suitable κ contribute LD with EOF to operate more robust in the P1 state. In this case, the LD generate a microwave photonic signal which can be used for achieving high performance sensing. As an application example, we built a displacement sensing experimental system. Both waveform and frequency of the MWP sensing signal contain the displacement information to be measured. Hence, we can achieve both integer and fractional fringe measurements. This work contributes to designing a prototype of a compact displacement sensor by using MWP in cooperate with OFI configuration to achieve wide measurement range, high sensing sensitivity, and high resolution.

References

[1] R. Lang and K. Kobayashi, "External optical feedback effects on semiconductor injection laser properties," *IEEE Journal of Quantum Electronics*, vol. 16, no. 3, pp. 347-355, 1980.

[2] M. C. Soriano, J. García-Ojalvo, C. R. Mirasso, and I. Fischer, "Complex photonics: Dynamics and applications of delay-coupled semiconductors lasers," *Reviews of Modern Physics*, vol. 85, no. 1, pp. 421-470, 03/20/ 2013.

[3] S. Donati, "Developing self-mixing interferometry for instrumentation and measurements," *Laser & Photonics Reviews*, vol. 6, no. 3, pp. 393-417, 2012.

[4] A. Uchida, *Optical communication with chaotic lasers: applications of nonlinear dynamics and synchronization*. John Wiley & Sons, 2012.

[5] O. D. Bernal, U. Zabit, and T. M. Bosch, "Robust Method of Stabilization of Optical Feedback Regime by Using Adaptive Optics for a Self-Mixing Micro-Interferometer Laser Displacement Sensor," *IEEE Journal of Selected Topics in Quantum Electronics*, vol. 21, no. 4, pp. 336-343, 2015.

[6] T. Taimre, M. Nikolić, K. Bertling, Y. L. Lim, T. Bosch, and A. D. Rakić, "Laser feedback interferometry: a tutorial on the self-mixing effect for coherent sensing," *Advances in Optics and Photonics*, vol. 7, no. 3, pp. 570-631, 2015/09/30 2015.

[7] V. Contreras, H. Martinez, and M. Norgia, "Phase Shift Measurements Between Intensity and Frequency Modulations of a Self-Mixing Interferometer," *IEEE Photonics Technology Letters*, vol. 30, no. 22, pp. 1909-1912, 2018.

[8] D. Guo, H. Jiang, L. Shi, and M. Wang, "Laser Self-Mixing Grating Interferometer for MEMS Accelerometer Testing," *IEEE Photonics Journal*, vol. 10, no. 1, pp. 1-9, 2018.

[9] J.-X. Dong, J.-P. Zhuang, and S.-C. Chan, "Tunable switching between stable and periodic states in a semiconductor laser with feedback," *Optics letters*, vol. 42, no. 21, pp. 4291-4294, 2017.

[10] P. Zhou, F. Zhang, Q. Guo, S. Li, and S. Pan, "Reconfigurable radar waveform generation based on an optically injected semiconductor laser," *IEEE Journal of Selected Topics in Quantum Electronics*, vol. 23, no. 6, pp. 1-9, 2017.

[11] P. Zhou, F. Zhang, X. Ye, Q. Guo, and S. Pan, "Flexible frequency-hopping microwave generation by dynamic control of optically injected semiconductor laser," *IEEE Photonics Journal*, vol. 8, no. 6, pp. 1-9, 2016.

[12] H. Chen, B. Nakarmi, M. R. Uddin, and S. Pan, "Optical Behavior Analysis of Negative Wavelength Detuning in SMFP-LD and Its Effect on Multi-RF Generation," *IEEE Photonics Journal*, vol. 11, no. 1, pp. 1-9, 2019.

[13] S.-C. Chan, S.-K. Hwang, and J.-M. Liu, "Period-one oscillation for photonic microwave transmission using an optically injected semiconductor laser," *Optics Express*, vol. 15, no. 22, pp. 14921-14935, 2007.

[14] X. Qi and J. Liu, "Photonic Microwave Applications of the Dynamics of Semiconductor Lasers," *IEEE Journal of Selected Topics in Quantum Electronics*, vol. 17, no. 5, pp. 1198-1211, 2011.

[15] C. Cui and S.-C. Chan, "Performance analysis on using period-one oscillation of optically injected semiconductor lasers for radio-over-fiber uplinks," *IEEE Journal of Quantum Electronics*, vol. 48, no. 4, pp. 490-499, 2012.

[16] L. Fan *et al.*, "Subharmonic Microwave Modulation Stabilization of Tunable Photonic Microwave Generated by Period-One Nonlinear Dynamics of an Optically Injected Semiconductor Laser," *Journal of Lightwave Technology*, vol. 32, no. 23, pp. 4660-4666, 2014.

[17] L. Li, X. Yi, S. X. Chew, S. Song, L. Nguyen, and R. A. Minasian, "Double-pass microwave photonic sensing system based on low-

coherence interferometry," *Optics letters*, vol. 44, no. 7, pp. 1662-1665, 2019.
[18] S. D. Cohen, A. Aragoneses, D. Rontani, M. Torrent, C. Masoller, and D. J. Gauthier, "Multidimensional subwavelength position sensing using a semiconductor laser with optical feedback," *Optics letters*, vol. 38, no. 21, pp. 4331-4334, 2013.
[19] V. Annovazzi-Lodi, S. Merlo, M. Norgia, and A. Scirè, "Characterization of a chaotic telecommunication laser for different fiber cavity lengths," *IEEE journal of quantum electronics*, vol. 38, no. 9, pp. 1171-1177, 2002.
[20] A. Zhao, N. Jiang, S. Liu, C. Xue, and K. Qiu, "Wideband Time Delay Signature-Suppressed Chaos Generation Using Self-Phase-Modulated Feedback Semiconductor Laser Cascaded With Dispersive Component," *Journal of Lightwave Technology*, vol. 37, no. 19, pp. 5132-5139, 2019.
[21] C. Bes, G. Plantier, and T. Bosch, "Displacement measurements using a self-mixing laser diode under moderate feedback," *IEEE Transactions on Instrumentation and Measurement*, vol. 55, no. 4, pp. 1101-1105, 2006.
[22] Y. Fan, Y. Yu, J. Xi, and J. F. Chicharo, "Improving the measurement performance for a self-mixing interferometry-based displacement sensing system," *Applied Optics*, vol. 50, no. 26, pp. 5064-5072, 2011/09/10 2011.
[23] M. Wang, "Fourier transform method for self-mixing interference signal analysis," *Optics & Laser Technology*, vol. 33, no. 6, pp. 409-416, 2001.
[24] Y. Tan, W. Wang, C. Xu, and S. Zhang, "Laser confocal feedback tomography and nano-step height measurement," *Scientific reports*, vol. 3, p. 2971, 2013.
[25] B. Liu, Y. Yu, J. Xi, Q. Guo, J. Tong, and R. A. Lewis, "Displacement sensing using the relaxation oscillation frequency of a laser diode with optical feedback," *Applied Optics*, vol. 56, no. 24, pp. 6962-6966, 2017/08/20 2017.
[26] Y. Ruan, B. Liu, Y. Yu, J. Xi, Q. Guo, and J. Tong, "High sensitive sensing by a laser diode with dual optical feedback operating at period-one oscillation," *Applied Physics Letters*, vol. 115, no. 1, p. 011102, 2019.
[27] Y. Ruan, B. Liu, Y. Yu, J. Xi, Q. Guo, and J. Tong, "Measuring Linewidth Enhancement Factor by Relaxation Oscillation Frequency in a Laser with Optical Feedback," *Sensors*, vol. 18, no. 11, p. 4004, 2018.

Bairun Nie received the B.E. degree in Telecommunications engineering from Zhengzhou University, China, and University of Wollongong, Australia, in 2017. The M.E. degree in Telecommunications engineering from University of Wollongong, Australia, in 2018. He is currently pursuing the Ph.D. degree in Signal Processing for Instrumentation and Communications Research Laboratory of University of Wollongong. His research interest includes self-mixing interferometry, laser sensing, and microwave photonics.

Yuxi Ruan received the B.E.(Hon) in Telecommunications engineering from University of Wollongong, Australia, in 2015. He is currently pursuing the Ph.D. degree in Signal Processing for Instrumentation and Communications Research Laboratory of University of Wollongong. His research interest includes optical feedback interferometry, optical sensing and laser dynamics.

Yanguang Yu received the B.E. degree from Huazhong University of Science and Technology, China in 1986, and Ph.D. degree from the Harbin Institute of Technology, China, in 2000, all in Electrical Engineering. She joined the University of Wollongong since 2007 and is now an Associate Professor at the School of Electrical, Computer and Telecommunications Engineering. She was with the Faculty of Information Engineering, Zhengzhou University, China, on various appointments including a Lecturer (1986-1999), Associate Professor (2000-2004), Professor (2005-2007). From 2001 and 2002 she was a Postdoctoral Fellow at Opto-Electronics Information Science and Technology Laboratory, Tianjin University, China. She also had a number of visiting appointments including a Visiting Fellow at the Optoelectronics Group, Department of Electronics, University of Pavia, Italy (2002-2003), a Principal Visiting Fellow at the University of Wollongong, Australia (2004-2005), a visiting Professor at the Engineering School ENSEEIHT, University of Toulouse, France respectively in June, 2004, September 2006 and June 2015. Yu has been working on non-contact optical sensing using optical feedback laser interferometer since her Ph.D. in 2000. Her research interests include sensing and measurements, 3-D profile measurements, signal processing and communication systems, and recently focus on microwave photonic sensing topic.

Qinghua Guo received the B.E. degree in electronic engineering and M.E. degree in signal and information processing from Xidian University, Xi'an, China, in 2001 and 2004, respectively, and the Ph.D. degree in electronic engineering from the City University of Hong Kong, Hong Kong, in 2008. He is currently an Associate Professor with the School of Electrical, Computer, and Telecommunications Engineering, University of Wollongong, Australia, and an Adjunct Associate Professor with the School of Engineering, University of Western Australia. His current research interests include signal processing and telecommunications.

Jiangtao Xi received the B.E. degree in electrical engineering from the Beijing Institute of Technology, China, in 1982, the M.E. degree in electrical engineering from Tsinghua University, China, in 1985, and the Ph.D. degree in electrical engineering from the University of Wollongong, Australia, in 1996. He was a Post-Doctoral Fellow with the Communications Research Laboratory, McMaster University, Hamilton, Canada, from 1995 to 1996, and a Technical Staff Member with Bell Laboratories, Lucent Technologies Inc. USA, from 1996 to 1998. In 2003, he rejoined the University of Wollongong, as a Senior Lecturer and he is currently a Full Professor and the Head of School of Electrical, Computer, and Telecommunications Engineering. His current research interests include signal processing and its applications in various areas, such as instrumentation and measurement, as well as communications.

Jun Tong received the B.E. and M.E. degrees from the University of Electronic Science and Technology of China (UESTC) in 2001 and 2004 respectively, and the Ph.D. degree in electronic engineering from the City University of Hong Kong in 2009. He is currently a Senior Lecturer with the School of Electrical, Computer, and Telecommunications Engineering, University of Wollongong, Australia. His research interest includes signal processing and its applications to communication systems.